Observations of the Inner Planets by the GOES Imagers and Application to the Calibration of the Advanced Baseline Imager's Thermal Infrared Channels

James C. Bremer[1],
Xianqian Wu[2],
J. Paul Douglas[3],
Michael P. Weinreb[4],
Hyre Bysal[2]

1. Research Support Instruments, Inc.
2. NOAA/NESDIS
3. Arctic Slope Research Corp.
4. Riverside Technology, Inc.

Why look at Mercury with the ABI?

- "Celestial targets are of particular interest --- for two reasons, 1) --- an independent check of on-board sensor calibration & 2) --- common targets for all earth & space-based instruments" [NOAA/NESDIS, "GOES-R Calibration and Validation Plan, Version 0.2" (2007)]
- Mercury has the following desirable attributes:
  - Virtually no atmosphere (blackbody-like IR spectrum with relatively little fine structure)
  - Angular diameter 25-50 μrad with varying phases
  - Hot sunlit surface with solid angle < ABI's thermal IR (TIR) pixels (56 μrad)^2
  - Irradiance within the useful dynamic range of most ABI TIR channels (7-16), but more highly weighted toward short wavelengths than the ICT (on-board blackbody)
  - Effective temperature increases rapidly with decreasing λ, providing sensitive test of spectral response functions (SRF's)
  - Observable in solar-reflective channels (1-6) with ~ 0-magnitude at 90^o phase
  - Co-observable from multiple platforms (Important for long-term climate trending)
  - Can be compared with multispectral/hyperspectral imagery of Mercury from Messenger (reflective bands only) & Bepi Colombo (reflective and TIR bands, after 2020)

[James C. Bremer, "On-board calibration of the spectral response functions of the Advanced Baseline Imager's thermal IR channels by observation of the planet Mercury", Proc. SPIE 7807, 78070M-1-12, (2010)]

Our observations of Mercury with the GOES Imagers during May, 2011 confirm the TIR irradiance predictions

ABI calibration, co-registration, & navigation will be challenging

Higher spatial, spectral, temporal & radiometric resolution than the Imager

Scan angle dependence of two-mirror scanner

Each mirror's reflectivity, polarization & SRF vary with angle
E/W scan moves optical beam footprint on N/S mirror
ICT only observed at $45^o/45^o$ reflection angles
ABI's Field-of-regard (FOR) limits space scans to short lines
Use sequential observations of Mercury on W & E sides of FOR to calibrate E/W variation

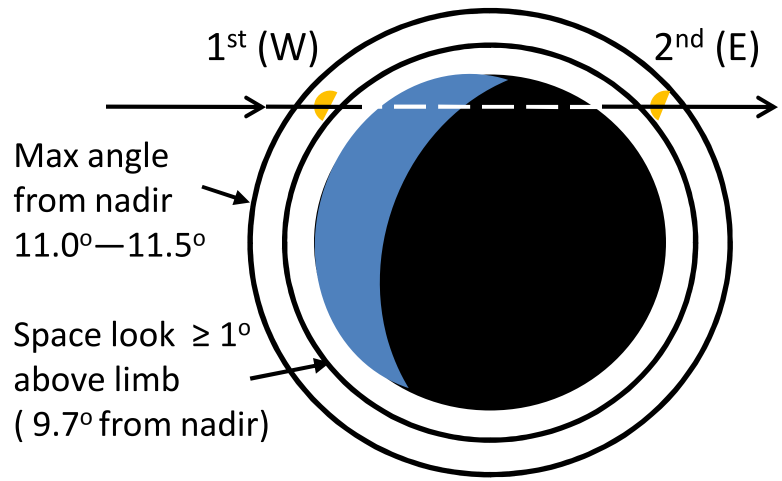

SRF's

"At the slope regions of atmospheric spectra, a small shift of the SRF can cause biases in observed radiances." [Ch 8-10 (H_2O), 12 (O_3) , & 16 (CO_2)]
Measure effective temperature of Mercury: $\delta\lambda/\lambda = -0.1\% \rightarrow \Delta T \cong +0.1K$

Co-registration of 16 long, linear arrays on 3 focal planes

Observe Mercury in all 16 channels

Long–term trending

Co-observe with instruments on other platforms to transfer calibration

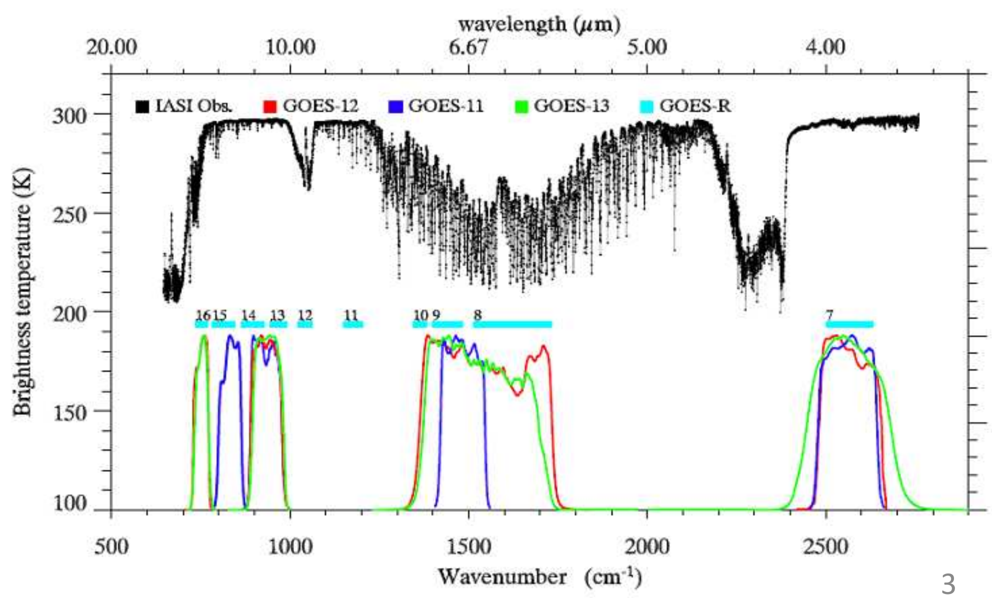

[Spectral diagram from GOES-R Cal/Val Plan]

Observations of Mercury by the GOES-11 (GOES-W) Imager in May 2011

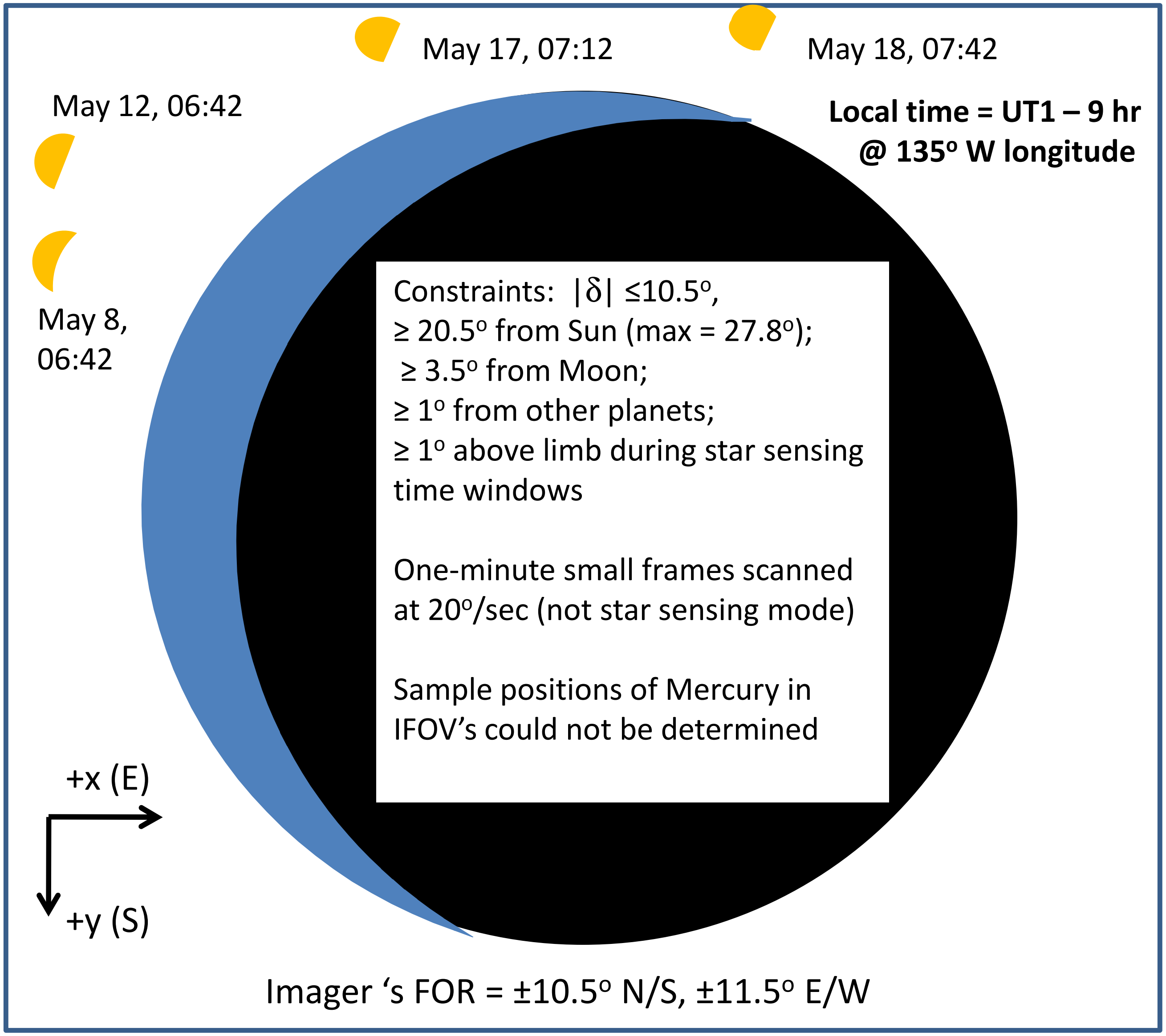

May 6, 06:42 UT1
(May 5, 2142 local)
D = 41 μrad,
ϕ = 103° (phase)
10.3° W, 4.7° N

May 8, 06:42 UT1
D = 39 μrad,
ϕ = 99°
10.2° W, 5.3° N

May 10, 06:42 UT1
D = 38 μrad,
ϕ = 95°
10.2° W, 6.1° N

May 12, 06:42 UT1
D = 36 μrad,
ϕ = 91°
10.4° W, 6.9° N

May 17, 07:12 UT1
D = 33 μrad,
ϕ = 82°
4.0° W, 9.3° N

May 18, 07:42 UT1
D = 33 μrad,
ϕ = 81°
3.2° E, 9.9° N

Model of Mercury's thermal IR emission

Nine sunlit zones with solar zenith angles, $\theta_k = k*10^o - 5^o$, k = 1-9
Each zone absorbs 94% of solar radiation & re-radiates as a blackbody
$T_k = (387.9\ K)(\cos \theta_k)^{1/4} d_s^{-1/2}$; d_s = Mercury-Sun distance (AU)

"Zone #"	"Zenith Angle (deg)"	"T(K)"	"Solid Angle (urad^2)"
1	5	594.8	3.8
2	15	590.2	12.9
3	25	580.9	26.4
4	35	566.4	42.6
5	45	545.9	59.4
6	55	518.1	74.9
7	65	480	87.2
8	75	424.6	94.8
9	85	323.5	96.8

Model of Mercury on May 17, 2011
D = 33 μrad, phase angle = 81.6°
Derived temperatures & observed solid angles of 9 zones

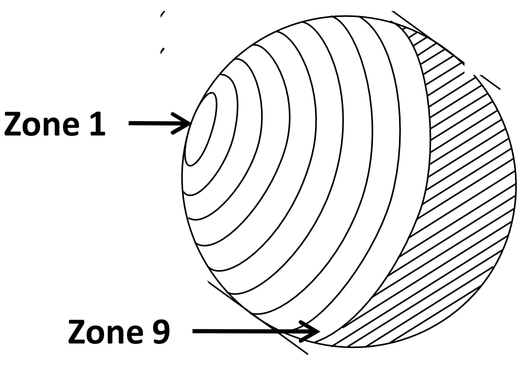

Comparison of irradiance levels of Mercury on May 17 (– – –) & the ICT (······) at 290 K in the GOES-11 (GOES-West) Imager's TIR Channels

IFOV's Ch 2: (112 μrad)^2 3.90 μm Ch 3: (224 μrad)^2 6.75 μm Ch 4: (112 μrad)^2 10.73 μm Ch 5: (112 μrad)^2 12.00 μm

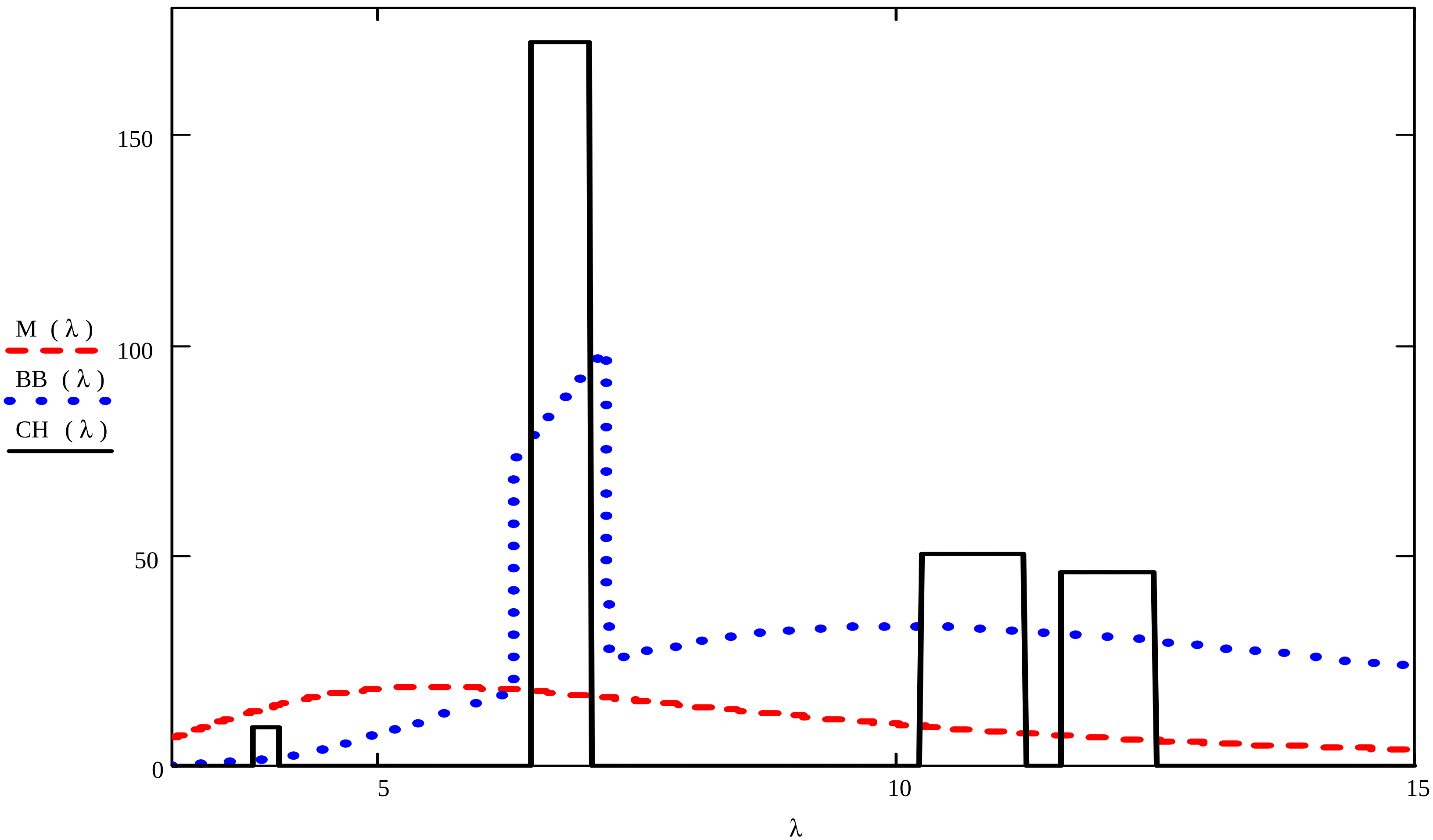

Estimated effective temperature of Mercury: May 17, 2011, GOES-W (G-11)

delT = change in effective temperature for $\delta\lambda/\lambda = -0.1\%$

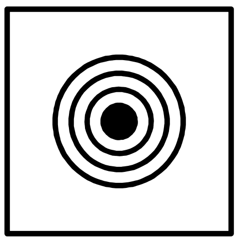

Eff T for centered Airy disk

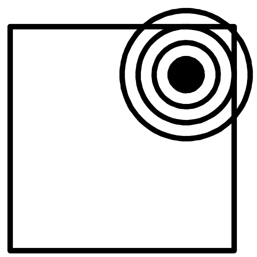

T decenter for Airy disk decentered (¼ IFOV)/axis

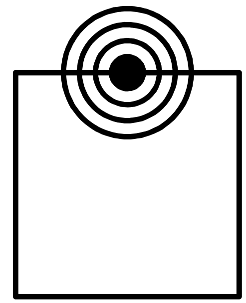

T straddle for Airy disk at edge of IFOV

Position of Mercury in Imager's IFOV's is unknown

IFOV = (224 μrad)^2 in Ch 3 & (112 μrad)^2 in all other TIR channels
Effective temperatures expected to lie in the range (T straddle – Eff T)

"Channel"	"λ (um)"	"Max T (K)"	"Eff T (K)"	"delT (K)"	"T decenter (K)"	"T straddle (K)"
2	3.9	335	348.22	0.12	347.62	327.09
3	6.75	320	236.92	0.13	236.47	220.15
4	10.73	320	220.19	0.12	218.63	198.57
5	12	320	206.65	0.11	204.76	185.72

Comparison of effective temperatures (K) of Mercury predicted & observed by the GOES-11 (GOES-W) Imager

[Time in UT1; local time 9 hrs earlier]

observed effective temperatures – (predicted T range)

Ch 2, 4, & 5: IFOV = (112 μrad)^2

Ch 3: IFOV = (224 μrad)^2

Date	May 6 [06:42, 06:43]	May 8 [06:42, 06:43]	May 10 [06:42, 06:43]	May 12 [06:42, 06:43]	May 17 [07:12, 07:13]	May 18 [07:42, 07:43]
Ch 2 3.90 μm	**311.6, 317.2** (309.8-328.2)	**306.5, 322.1** (313.0-331.7)	**311.9, 318.7** (315.9-335.0)	**325.5, 328.0** (319.0-338.5)	**311.6, 341.2** (327.1-347.6)	**330.6, 341.2** (328.8-349.6)
Ch 3 6.75 μm	**218.0, 216.6** (211.5-226.6)	**212.5, 208.4** (213.2-228.4)	**220.0, 211.2** (214.7-230.2)	**207.3, 223.8** (216.2-231.9)	**229.1, 229.6** (220.2-236.5)	**230.2, 230.5** (221.0-237.4)
Ch 4 10.73 μm	**188.4, 189.0** (190.9-209.4)	**189.6, 191.5** (192.5-221.3)	**190.3, 191.5** (193.9-212.9)	**197.5, 196.5** (195.2-214.5)	**193.2, 203.2** (198.6-218.6)	**202.3, 199.0** (199.3-219.5)
Ch 5 12.00 μm	**171.4, 175.1** (178.9-196.5)	**178.4, 182.0** (180.2-198.1)	**175.7, 179.0** (181.4-199.6)	**179.0, 182.6** (182.6-201.1)	**173.7, 187.9** (185.6-204.7)	**186.3, 189.3** (186.3-205.5)

[Michael P. Weinreb, Joy X. Johnson, & Dejiang Han, "Conversion of GVAR Infrared Data to Scene Radiance or Temperature", http://www.oso.noaa.gov/goes/goes-calibration/gvar-conversion.htm]

Comparison of irradiance levels of Mercury on May 17 (- - -) & the ICT (······) at 290 K in the GOES-13 (GOES-East) Imager's TIR Channels

IFOV's	Ch 2: (112 μrad)^2	Ch 3: (112 μrad)^2	Ch 4: (112 μrad)^2	Ch 6: (224 μrad)^2
	3.90 μm	6.57 μm	10.67 μm	13.34 μm

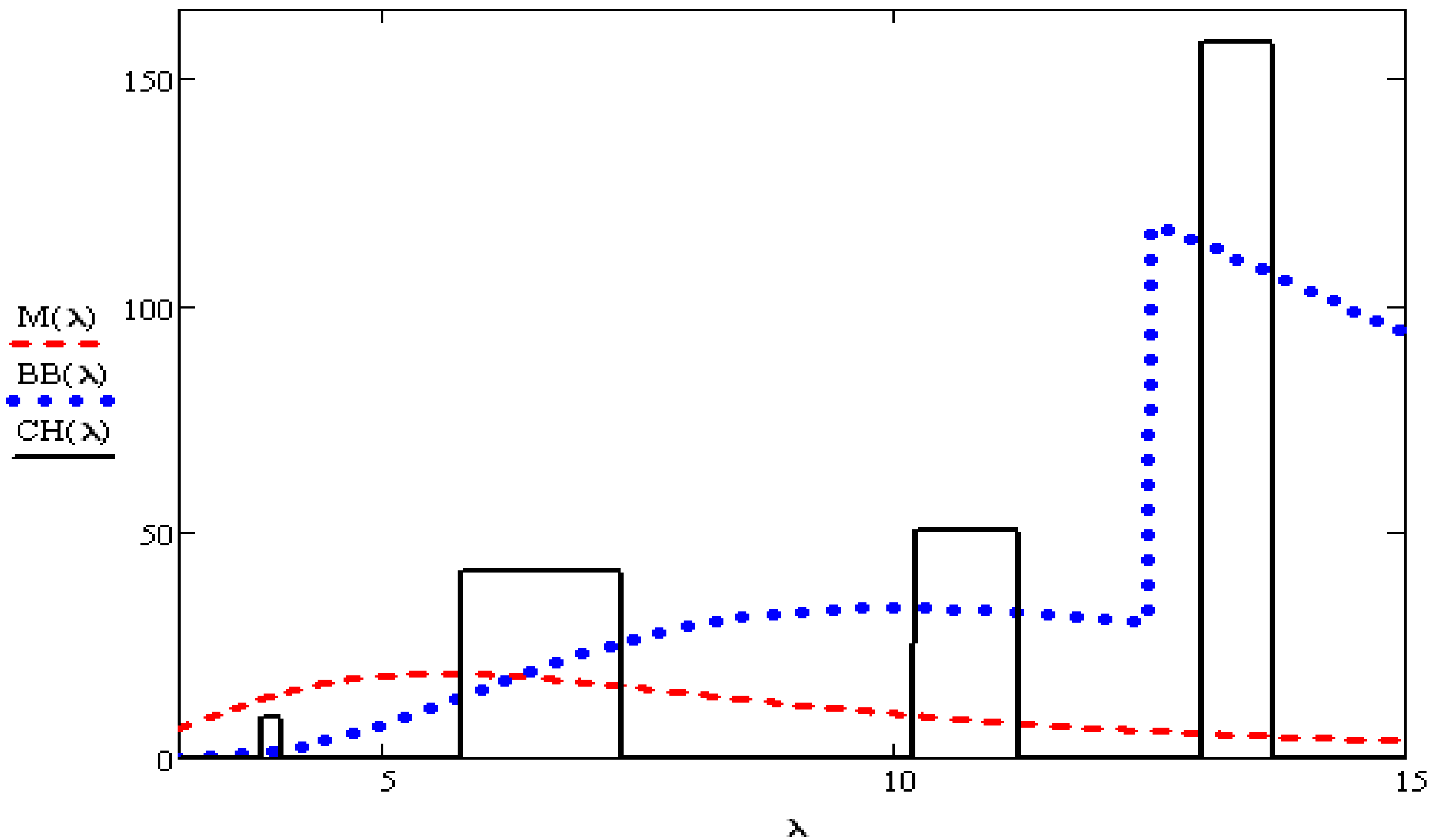

Comparison of effective temperatures (K) of Mercury predicted & observed by the GOES-13 (GOES-E) Imager

[Time in UT1; local time 5 hrs earlier]

observed effective temperatures – (predicted T range)

Ch 2, 3, & 4: IFOV = (112 μrad)^2

Ch 6: IFOV = (224 μrad)^2

Date	May 17 [04:07]	May 19 [04:07]
Ch 2 3.90 μm	**328.6** (327.1-347.6)	**319.2** (330.6-351.6)
Ch 3 6.57 μm	**263.7** (259.4-280.8)	**266.7** (261.8-283.5)
Ch 4 10.67 μm	**210.6** (199.3-219.4)	**197.6** (200.7-221.1)
Ch 6 13.34 μm		**151.0** (144.3-157.8)

[Michael P. Weinreb, Joy X. Johnson, & Dejiang Han, "Conversion of GVAR Infrared Data to Scene Radiance or Temperature", http://www.oso.noaa.gov/goes/goes-calibration/gvar-conversion.htm]

Effective temperatures (K) of Venus

GOES-11 (GOES-West)

GOES-12 (GOES South America)

[Time in UT1; local time 9 hrs earlier for GOES-11 & 4 hrs earlier for GOES-12]

Date	May 17 [07:13]
Ch 2 (112 μrad)^2 3.90 μm	**341.4**
Ch 3 (224 μrad)^2 6.75 μm	**338.6**
Ch 4 (112 μrad)^2 10.73 μm	**392.8**
Ch 5 (112 μrad)^2 12.00 μm	**436.6**

Date	May 17 [03:12]	May 19 [03:12]
Ch 2 (112 μrad)^2 3.90 μm	**337.0**	**337.0**
Ch 3 (112 μrad)^2 6.51 μm	**322.2**	**322.3**
Ch 4 (112 μrad)^2 10.72 μm	**377.2**	**377.3**
Ch 6 (224 μrad)^2 13.30 μm	**430.9**	**431.1**

[Michael P. Weinreb, Joy X. Johnson, & Dejiang Han, "Conversion of GVAR Infrared Data to Scene Radiance or Temperature", http://www.oso.noaa.gov/goes/goes-calibration/gvar-conversion.htm]

“Goldilocks” Chart for Celestial Targets in the Imager’s TIR Channels

Too hot (T_{eff} > T_{max}), Too cold (T_{eff} < 180 K), Just Right (180 K < T_{eff} < T_{max})

Channel Satellite	2 All	3 G-12/13	3 G-11	4 All	5 G-11	6 G-12/13
Nominal λ (μm)	3.9	6.5	6.75	10.7	12.0	13.3
IFOV (μrad)	112x112	112x112	224x224	112x112	112x112	224x224
T_{max} (K)	335	320	320	320	320	320
Moon						
Mercury						
Venus						
Jupiter						
Other planets						
Betelgeuse (?)						
Other stars |δ| < 10.5°						

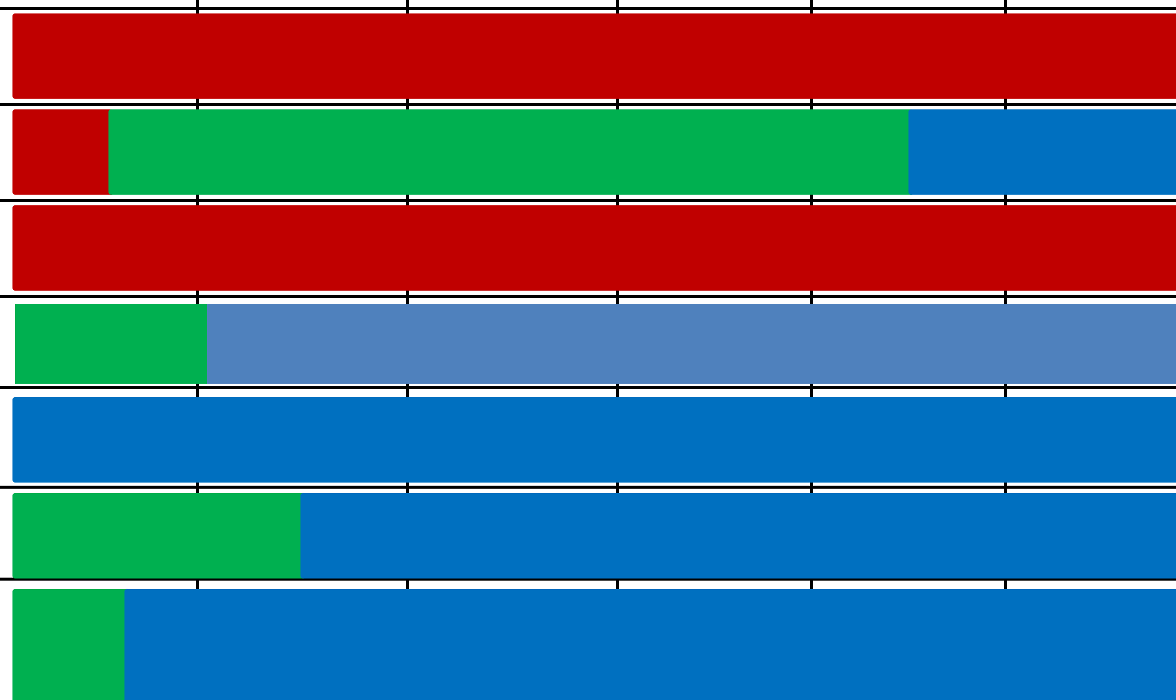

Application to the ABI

Observation of Mercury ---

- is a sensitive technique for detecting SRF deviations in TIR channels
  - Effective T within useful dynamic range of most TIR channels
  - Effective T near top of 3.9 μm channel's dynamic range (400 K)
  - SRF $\Delta\lambda/\lambda$ = - 0.1% produces $\Delta T \approx + 0.1$ K, comparable to NEΔT in most ABI TIR channels
- can be used to minimize image defects due to non-uniformity
  - Variation among detector elements within a spectral channel (causes striping)
  - Variation with scan mirror angle from west to east in FOR (causes shading)
- is an effective method of cross calibration among reflective & TIR channels of different spaceborne instruments
- can verify co-registration among all channels, especially TIR channels in atmospheric absorption bands (augmenting 0.64 μm/3.9 μm star co-observations)
  - An extended source is preferable to a point source for centroid measurements
  - Mercury's irradiance is great enough for LWIR measurements
- can be implemented with minor modifications to existing observational modes

Observation of Venus would saturate the ABI's TIR channels at λ > 3.9 μm, but is potentially a good technique for instruments with larger IFOV's

Acknowledgements

- This effort was supported in part by NASA contract NNG07CA21C & in part by RSI, Inc.
- We would like to thank the following individuals for their assistance:
  - Dr. H. John Wood, NASA/GSFC
  - Dr. Changyong Cao, NOAA/NESDIS
  - Mr. Dane Evans, ASRC, Inc.
  - Ms. Fangfang Yu, ERT, Inc.
  - Mr. Kenneth Mitchell, ASRC, Inc.

False event rejection

(backup)

- Probability of false event due to charged particles $\cong 10^{-5}$/pixel
- No correlation between false alarms in different channels
- No correlation between false alarms in consecutive frames
- Require detections in two or more channels in the same area of the same frame or detections in the same channel in the same area of the frame in two consecutive frames

Upcoming time windows for observations of Mercury and Venus with the Imager

(backup)

| Declination | ≤ 10.5°; Elongation ≥ 20.5°

(Lunar & planetary avoidance may impose additional constraints)

Mercury	Venus (2012 only)
2012: April 4 - May 7	2012: present-March 1
2013: March 17-April 20	2012: Oct. 6-Nov 23
2013: Sept. 22 - Sept.24	
2014: March 25 - April 3	
2014: Sept. 3 - Sept. 18	
2015: August 16 - Sept. 18	

Quote from Cal/Val Plan

(backup)

“---spectral shift in response due to temperature changes, contaminant deposition on the front mirrors, and radiation aging of previously chosen mirror coatings, have been identified as major sources of SRF uncertainties on orbit. “